Measuring Holocene soil redistribution on the flanks of the Ootmarsum ice-pushed ridge – using OSL

Duco de Vries

MSc thesis

March 2016

Title:

Measuring Holocene soil redistribution on the flanks of the Ootmarsum ice-pushed ridge – using OSL

Author:

Duco de Vries

Supervisors:

Tony Reimann

Jeroen Schoorl

Soil Geography and Landscape Group

Wageningen University

the Netherlands

March 2016

Cover painting:

A Watermill besides a Woody Lane

By Meyndert Hobbema, 1665 (Amsterdam 1638 - Amsterdam 1709)

Abstract

Anthropogenic land use and habitation of the ice-pushed ridge of Ootmarsum started early in the Holocene. The early cultivation of this area could have influenced soil stability and thus have induced soil erosion. In this study, colluvial layers in two valley positions were sampled at different depths and dated using OSL dating. In both valley sampling positions, a peaty layer was found on top of well-sorted fine sand, which initially was thought to be Weichsel coversand. As the catchments in the study area are small, the erosion-deposition distance is short and thus the chance of incomplete bleaching increases. The sampled material was dated on small aliquots (~12 and ~49 grains), as a proxy for single grain measurements. For most samples, the un-logged version of the Minimum Age Model was used to estimate the burial age. The resulting MAMul ages show stratigraphic consistency and even the youngest samples match well with an independent age check of Caesium (^{137}Cs).

The results show that soil erosion reached a climax in the late Middle Ages. Land use intensity was high during this period: sediments where redistributed for *plaggen* fertilization and the hydrology was adapted for the use of watermills. No colluvium was found dating from the period between the end of the Weichsel and the Middle Ages but this does not exclude the possibility of soil erosion in this period; colluvium dating from this period could have been bleached, eroded or removed.

Contents

1. Introduction

During the past decennia, sediment dynamics and soil redistribution in relation to land use are studied extensively for undulating areas. However, most studies are only limited to relatively short timescales and do not focus on past dynamics and land use history.

The ice-pushed ridge near Ootmarsum, in the east of the Netherlands, is prone to erosion due to its relative elevation in the landscape and is known to have had a quite active land use and habitation history. Archaeological studies have indicated that agricultural cultivation in the area of Ootmarsum started already in the beginning of the Holocene (van Beek et al. 2015). The ice-pushed ridge consists mostly of sandy glacial sediments pushed up by glacial movement in the Saale Period. Anthropogenic land use has been a prominent trigger of erosion in several hilly to mountainous areas during the Holocene (Lang and Hönscheidt 1999a; Lang 2003; Schmitt et al. 2003; Fuchs et al. 2004; García-Ruiz 2010). However, the ice-pushed ridge of Ootmarsum does not have very steep slopes, averagely around 2°. This raises the question whether these slopes are steep enough for small scale agriculture to cause erosion. The relation between anthropogenic land use during the Holocene and soil erosion and deposition is not studied before in this area.

On the lower eastern flanks of the ice-pushed ridge, colluvial sedimentation layers exist in several small valleys (see Figure 2.3). These layers can be found on top of Weichsel coversands, indicating they are deposited afterwards, in the Late Glacial or Holocene. Recent studies prove that colluvium can be a valuable sedimentary archive for paleo-environmental and geomorphological research, especially for reconstructing the landscape response to climate and anthropogenic induced soil erosion (Dotterweich 2008; Augustsson et al. 2013). The most important hillslope processes causing colluvium, a general term for sediments deposited at the base of hillslopes, are soil erosion (e.g. ploughing, sheet and rill erosion), mass movements (e.g. sliding, falling) and soil creep (e.g. solifluction) (Fuchs and Lang 2009).

Figure 1.1. Location of the ice-pushed ridge of Ootmarsum, indicated in red.

First signs of agricultural land use in the east of the Netherlands originate from the early Neolithic (van Beek et al. 2015). Land use in this region has changed gradually from forest during the early Holocene, to an open landscape with arable farming in present days, with a climax in land use and habitation intensity in the Middle Ages. Because of the early start of agriculture in the area around the ice-pushed ridge, the presumption exists anthropogenic land use may have had an impact on soil stability and could have induced soil erosion since the Neolithic.

Not only land use dynamics could have influenced soil stability; Holocene climate fluctuations may also triggered or boosted hillslope processes (Leopold and Völkel 2007; Schneider et al. 2007; Dotterweich 2008).

For dating colluvial material and establishing a burial chronology, luminescence dating is the most preferred technique in this study, because with this method the actual date of burial is measured.

Radiocarbon (^{14}C) dating would be less suitable, as this method dates the death of an organism and thus determines the first time sediments entered the cycle of soil redistribution (Lang and Hönscheidt 1999a; Fuchs and Lang 2009).
The aim of this study is dating the colluvial layers in the valleys of the ice-pushed ridge of Ootmarsum, to obtain a robust sedimentation chronology and evaluating the possible relationship between erosion intensity, land use and climate during the Holocene. Optical Stimulated Luminescence dating (OSL) is used to date the burial age of the colluvium. Although OSL dating is the most suitable technique for dating colluvium, dating sediments with such a short displacement distance is unique. Dating the colluvium in the study area is therefore one of the major challenges.

For this study, several research questions are posed to support the main goals. The main research question is: *What is the timing of soil redistribution during the Holocene on the Ootmarsum ice-pushed ridge and what are the main causative factors?* To answer this question, several sub-questions are posed:

- What is the most convenient method for OSL dating of Holocene colluvium with a high change of poor bleaching?
- What has been the impact of Holocene climate fluctuations on soil erosion and deposition at the ice-pushed ridge of Ootmarsum?
- What has been the impact of anthropogenic land use during the Holocene on soil erosion and deposition at the ice-pushed ridge of Ootmarsum?

In the next sections the landscape genesis and the history of the agricultural land use and habitation of Ootmarsum will be introduced.

2. Study area

2.1. *Landscape genesis*

Land ice reached up to the Netherlands during the Saale Glacial, pushing up Tertiary and Pleistocene sediments and debris. The moving ice-mass pushed up sediments creating an imbricated structure, consisting alternatingly of Tertiary clays and sands and Pleistocene River sands. Eventually, the ice mass glided over the sediments creating layers of glacial till, which are still present in the subsoil of the ice-pushed ridge.

During the Weichsel, the last geological glacial period, the Scandinavian continental ice-sheet did not reach up to the Netherlands. However, the study area was influenced by periglacial low temperatures. North Europe showed a tundra like climate and must have looked like an arctic desert with low vegetation density. During a significant part of this glacial period, permafrost was present, influencing the permeability of the soil. Surface runoff emerged due to the low permeability of the soil resulting in increased erosion rates. Small valley systems developed and incised into the ice-pushed ridge, like the valley of the *Springendal* in the study area. The top soil was thawed during summer, creating the ideal circumstances for solifluction, which leads again to flattening of the relief (Gans 1983).
The temperature and humidity fluctuated during this last ice-age with stadials (colder) and interstadials (warmer) and wet and drier periods (Zonneveld 1980). During drier periods, stadials, there was less vegetation and the wind could easily blow and replace sediments. During these periods, large belts of aeolian deposits covered North-West Europe in several phases (Old coversand to Young coversand) (Kolstrup 2007).
In the Late-Glacial interstadials, *The Bølling* and *the Allerød*, temperatures were relatively high and peat growth occurred on a large scale. After the *Allerød* interstadial, a stadial occurred (*Late Dryas*) with large coversand deposits (young coversand II) (G. Ebbers and R.Visscher 1992).
These coversands have lacking or very small humus layers, which is typically for the periglacial deposition conditions. (van den Berg and Den Otter 1982; Jongmans et al. 2012). A new climatic period started around 10.000 years ago, the Holocene. The climate became warmer again, vegetation recovered and soils started to develop in the pushed-up sediments. Characteristic Holocene formations consist of river and stream deposits, peat and drift-sands (G. Ebbers and R.Visscher 1992).

2.2. *Land use and habitation history*

During the late Palaeolithic (circa 10.500-7.000 BC), small groups of hunter-gatherers were roaming through North-West Europe. Late Palaeolithic sites can be found in the East of the Netherlands, on the sandy slopes of the ice-pushed ridges (van Beek et al. 2015). During this period, also called the Pre-Boreal, vegetation still recovered from the last glacial period; forests were expanding, containing birches, pines, poplars and carr in the wet brook valleys (Bouman et al. 2013).
The human influence on the landscape was limited in the early Neolithic period (circa 4000 BC). During the Atlanticum, deciduous forest developed over whole Twente and bogs were starting to grow.
During the Sub-Boreal, the middle Neolithic Funnel Beaker Culture moved into the area (3400-2750 BC), which is clearly recognisable in archaeological and pollen records (Kalis et al. 2003; Spek 2004). Settlements from this period are generally found on the flanks of the ice-pushed ridges and on lower moist areas, which were probably characterised by deciduous forests. Only a few settlements are found on top of the ice-pushed ridges (van Beek et al. 2015). These culture did not settle at one place but still roamed around, creating open spots in the forests for small-scale agriculture (Bouman et al. 2013). Kalis et al. (2003) concluded for a study in Germany that due to new agricultural techniques as ploughing and new crops erosion and deposition of sediments increased.
In the beginning of the Sub-Atlanticum, the Roman period, deforestation occurred on a much larger scale and an open forest developed on the ice-pushed ridge. During this period, the land within the study area was dominantly cultivated with cereal, which is also represented in pollen-diagrams (Bouman et al. 2013; van Beek et al. 2015).
According to van Beek and Bouman, the area was largely deforested by the end of the Middle Ages (circa 1500 AD) and used for agricultural purposes. Forest remained only high on the ice-pushed ridge. In the valleys, the carr disappears and is being replaced by meadow.
Nowadays, the east of the Netherlands is a very open landscape containing mostly heathland, grassland and agriculture. Pine forests have returned because of replantation since the 19th century (Bouman et al. 2013).

The Middle Ages influenced the soil properties in the study area extensively. The development of man-made soils (*Plaggen soils*) started around the 14th century (Mücher et al. 1990). These soils were fertilised with a mixture of manure, sods, litter and sand for centuries and are still clearly visible in the landscape (Mücher et al. 1990). The original underlying soil is often a Podzol (moder or humus Podzol) or a hydromorphic sandy soil (Pape 1970). When their *plaggen* layer is 50 cm or thicker, these soils are classified as Plaggic Anthrosol (WRB 2006) or *Enk* earth soils according to the Dutch system of soil classification. Large areas of the ice-pushed ridge are classified as *Enk* Soils which are represented in Appendix A (*Hoge bruine Enkeerdgronden; lemig fijn zand, Hoge zwarte Enkeerdgronden; leemarm en zwak lemig fijn zand, Hoge zwarte Enkeerdgronden; lemig fijn zand*). The material of the plaggen in this region mostly consists of material originating from coversand regions and small brooklets in the surrounding (Mücher et al. 1990).

Because there are several valleys in the ice-pushed ridge where natural sources rise, this was the ideal location for the usage of hydropower. Watermills have been widely present during the Middle

Ages in this area (Hagens 1979) as well around 50 meters upstream of sample location A (see Figure 2.1 and Figure 2.2).

Mills are seldom found individual along a water source, mostly there were several along a stream. In present days, most of the mills have disappeared, but the former watermills can still be found in old maps and writings. The influence of milling on soil redistribution could have been substantial; milling directly influences the geomorphological behaviour of streams and influences sediment load carrying capacity. Damming the valley bottoms to create a water reservoir and a bigger gradient for hydropower, could have been a widespread cause of valley sedimentation (Walter and Merritts 2008). Stream velocity decreased upstream of the mill pond which created slack water, while the stream velocity increased downstream of the pond. Containing less sediment and having a higher velocity after the mill leads to the creating of a scour pool and erosion rates. During the active periods of the watermills, it was common practice to dredge and flush the mill ponds regularly to maintain its usage. Where mills and mill channel structures are abandoned, streams try to re-establish a new equilibrium which may include incision of the streambed and rapid sediment releases (Downward and Skinner 2005). From old documents of the city of Ootmarsum it is known that the streams in the area were maintained regularly. A transcription by Smeenge (Diss. in progress) presents a request from 1770 to the landowners and farmers to clean and dredge their ditches.

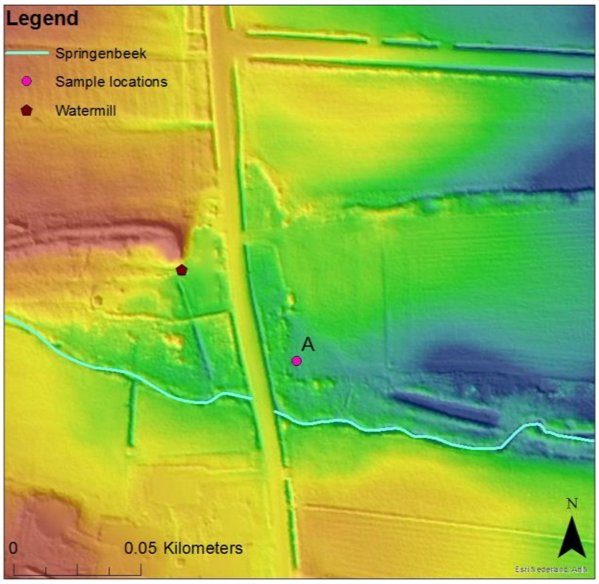

Figure 2.1. Sample location A in the Springendal. Showing a clearly visible remaining of a channelized river, possibly related to the upstream watermill. Base map is AHN2 0.5m

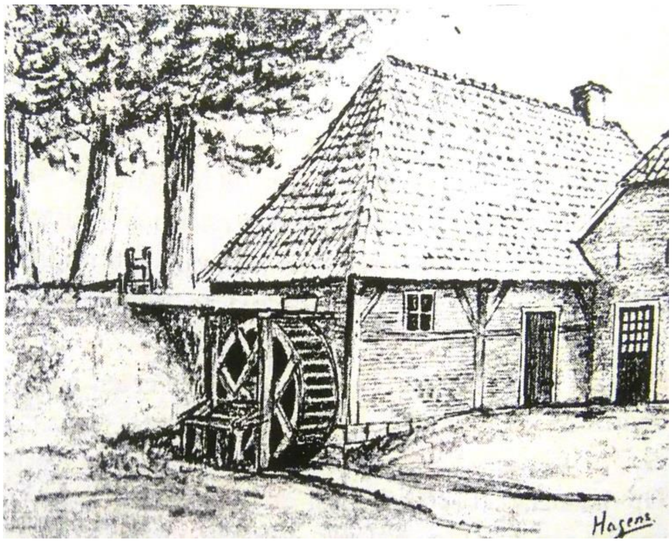

Figure 2.2. Drawing of the original watermill upstream of sample location A. De 'Bovenste molen van Cramer', drawing by Hagens (1979)

2.3. ***Soil and landscape characterisation***

The Tertiary ice-pushed deposits can mainly be divided in two lithological units: heavy clays (Boulder clays and Tertiary clays) and all other lithologies which are mainly loamy sands to loam (van den Berg and Den Otter 1982). The presence of impermeable clay layers near the soil surface explains the existence of wet soils and numerous springs around the ice-pushed ridge. Small brooklets and bog pools developed as a result of rising groundwater in the Holocene. In the sandy valleys, generally B*eekeerdgronden* are found. The valleys where peat is formed and deposited are classified as *Beekdalgronden* (G. Ebbers and R.Visscher 1992)*.* On the drier sandy soils mostly *Veldpodzolgronden* and *Holtpodzolgronden* formed. Large parts of these soils are used for *plaggen* fertilisation and are now classified as *Enkeerdgronden* (*s*ee Appendix A for an explanation of the Dutch soil classification).

Currently the most common land uses are meadows, arable lands (agricultural grass and maize) and deciduous forests.

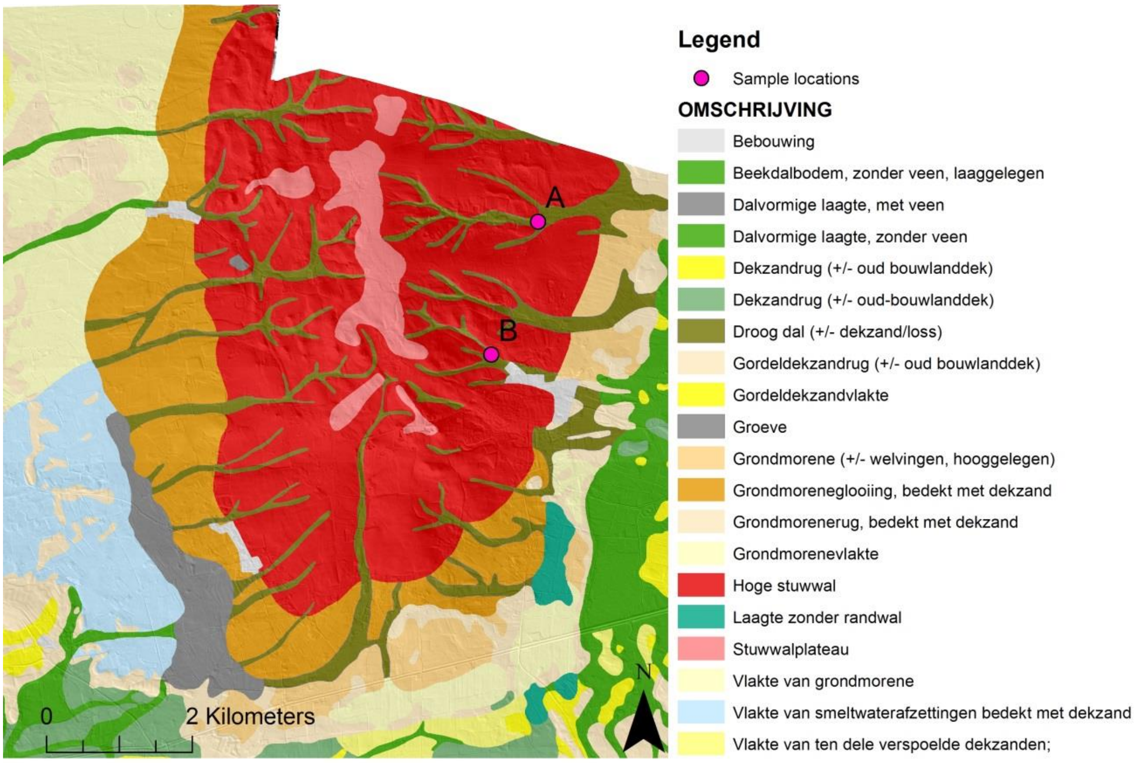

Figure 2.3. Fragment of the geomorphological map 1:50.000 of the study area (Alterra 2004)

3. Methods

3.1. *Soil and site description*

Colluvium is most likely to be found on the lower end of slopes. The slopes on the east side of the ice-pushed ridge are steepest, presumably because the land surface is pushed up from that direction (van den Berg and Den Otter 1982). Because the east side of the ice-pushed ridge consists of more sandy material compared to the west side and because the slopes are steeper, more erosion is expected on this flank.

The sampling has been carried out in the summer of 2015. Five potential locations to find colluvium were selected beforehand, based on satellite images and a Digital Elevation Model (Figure 3.1). In the field a soil survey was done at these locations by analysing soil borings (soil survey was done by dr. T. Reimann, dr. J.M. Schoorl and dr. A.J.A.M. Temme)

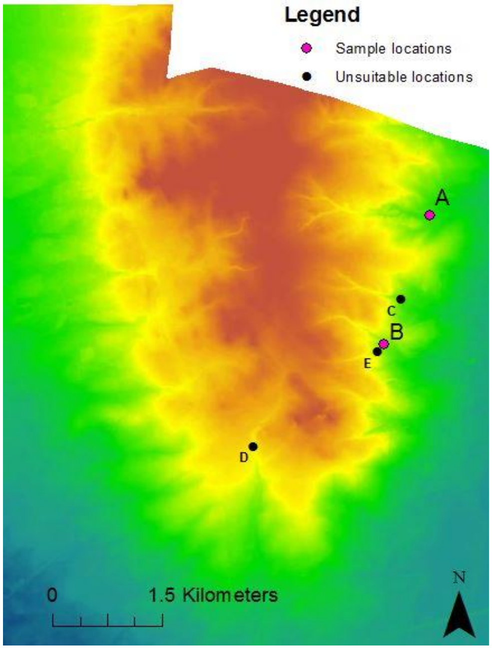

Figure 3.1. Sample locations for the luminescence dating. Base map is AHN2 5m

For location C, the farmer did not give permission to enter his field for soil observation. On locations D and E, there was no colluvial material found because the soil was reworked recently.

At the last two locations (A and B, Figure 3.1 and Figure 3.2) an organic, peaty layer was found on top of fine well-sorted sand. At both locations the peaty layer was stratified, which could have been caused by different depositional phases.

In the Springendal valley, location A, the peaty layer was a clear infilling of the old Weichsel valley. Light coloured Tertiary or Pleistocene sands were found in a valley-shaped position, in which the lower part was filled with organic rich sediment. At location B, the soil profile showed more clear evidence of recent ploughing and at a depth of 100-110 cm, peat remnants were found containing rests of birches. At the

Table 1. Sample depths and characteristics.

Field code	Sample nr.	Depth (cm)	Organic content (%)	Water content (%)
Location A				
A39_40	NCL-7315039	40	1.6%	22.7%
A40_50	NCL-7315040	50	2.4%	27.1%
A49_50	NCL-7315049	50	2.2%	22.0%
A50_58	NCL-7315050	58	2.7%	25.0%
A51_68	NCL-7315051	68	2.2%	24.6%
A52_80	NCL-7315052	80	1.9%	26.5%
A53_95	NCL-7315053	95	0.2%	14.2%
Location B				
B42_20	NCL-7315042	20	5.0%	22.9%
B43_35	NCL-7315043	35	5.6%	30.2%
B44_45	NCL-7315044	45	7.2%	37.2%
B45_60	NCL-7315045	60	6.9%	23.0%
B46_70	NCL-7315046	70	9.0%	54.9%
B47_100	NCL-7315047	100	5.7%	36.4%
B48_100	NCL-7315048	100	0.8%	21.6%

moment of sampling, in the summer of 2015, the land use of both locations was agricultural grass. For location A this was directly besides a maize field and a narrow strip of woodlands. Both sample locations are within several meters distance of the valley bottom and the corresponding stream. Of locations A and B, the upstream catchment areas are 2.2 km^2 and 0.8 km^2 respectively, calculated using the AHN2.

Figure 3.2. Soil pits of respectively sampling location A and B. Both soil profiles show a peat layer on top of well-sorted fine sands (below the groundwater table).

3.2. ***Sampling***

Sampling for OSL dating must be carried out with utmost precision to prevent sediments from bleaching during the sampling process. The OSL samples for this study, 15 in total, were taken from a vertical soil profile in a soil pit (see Figure 3.2). One sample was a bulk sample to test whether the result age could be in the hypothesised age range. PVC-tubes of approximately 21 x 4.5 (length x diameter) cm were hammered into the soil profile at heights between 20 and 100 cm. To sample colluvial layers of different depositional phases, sampling heights were chosen based on visual distinctive characteristics between layers such as grain size, sorting and colour. When the tubes were removed out of the soil profile the ends were closed and only reopened in the OSL laboratory under subdued orange light.

3.3. ***OSL Dating***

3.3.1. Introduction to dating of colluvium

Optical Stimulated Luminescence dating (OSL) is based on the principle that sediments contain a small amount of naturally occurring radioactive isotopes such as uranium, thorium or potassium-40. The sediments are subject to the same low amounts of radiation coming from these radioactive isotopes in their close surrounding. In the mineral crystals of quartz and feldspar grains, this leads to ionisation of atoms; freed electrons can move from the valence band to the conduction band. Normally these freed electrons leave the activated state and fall back to the valence band but some get trapped in electron traps, leaving a hole in the valence band. These electrons can be released when heated or exposed to (sun)light, which can be mimicked in a laboratory. When these electrons are released and recombined with a hole in the valence band, an emission of light occurs which is proportional to the amount of electrons that were trapped. The longer sediment is buried, the more electrons will get trapped (Walker and Walker 2005; Preusser et al. 2008).

The build-up radiation energy from quartz in this case, also called *equivalent dose* (D_e), is measured by use of OSL dating to determine the burial age. When a grain gets exposed to daylight (bleaching), this build-up signal resets. After burial, the grain will be charged again by the radiation of the environment, which is called *dose-rate* (D_r). To calculate the age of the last exposure to daylight, the equivalent dose must be divided by the radiation dose-rate (Preusser et al. 2008):

$$age\ [ka] = D_e\ [Gy] / D_r\ [Gy/ka] \quad (1)$$

The main requirements for OSL dating are (Murray and Wintle 2000):

- Competition for charge during trap filling is the same during laboratory irradiation as during natural irradiation.
- The OSL response is the same during measurement of both the natural and laboratory-induced signals.
- The traps are stable over the relevant geological time periods.
- The sediment grains have been bleached at time of burial.

A prerequisite for OSL dating is that sediment grains are exposed to sunlight long enough to completely reset the build-up energy. This is not always the case for colluvium; dating colluvium can give some difficulties, because the deposited sediments are transported via hillslope processes. Soil that moves downslope is often aggregated, whereby only the outer grains of the aggregation have a change for bleaching. In this study, the erosion-deposition distance is rather short, because the valleys are relatively small. The chance that the build-up energy in the grains has been completely zeroed at the time of deposition decreases because of a short exposure time (Preusser et al. 2008; Fuchs and Lang 2009). Although there are a lot of possible constraints, there are various examples illustrating that dating colluvium using OSL can be successful. Erosion and deposition are often gradual processes, whereby sediments are stored temporarily in sinks a little downslope before moving further downslope again. During these multiple erosion events, the chance of bleaching is higher (Lang and Hönscheidt 1999b). Ploughing and bioturbation also increases the chance of sufficient bleaching. If the colluvial activity is linked to anthropogenic land use, the chance of sufficient bleaching increases, which is the case for this study.

The deposition age of the colluvium in this study is relatively young for OSL dating, which can potentially result in a relatively high impact of incomplete bleaching. If the grains have been fully bleached, the individual equivalent doses will be tight and normally distributed. While for samples containing grains having different degrees of bleaching, the distribution will be broad and positively skewed (Olley et al. 1998). In this case, the distributions of paleodoses are positively skewed, in which the higher paleodoses are the ones that have not been fully reset at time of deposition.

3.3.2. Experimental details

The soil samples that have been taken were opened in the OSL lab of The Netherlands Centre for Luminescence dating (NCL) under subdued orange light. The outer 5 cm of the samples in the PVC-tubes were removed to avoid potential contamination during the sampling process. These outer sediments are only used for water, organic content and dose-rate measurements.

The samples were (wet) sieved and the 212-250 μm fraction was used for further analysis. To remove any carbonate and organic matter, the 212-250 μm grains were treated with HCl (10%) and H_2O_2 (10%). To remove any feldspars and remove the etches of the grains that have been influenced by alpha radiation, a standard treatment in hydrofluoric acid HF (10%) and HF (40%) was applied. And finally the sieved fraction was again treated with HCl (10%) to obtain a clean quartz extract.

The aliquots were measured using a Risø TL/OSL-DA-15 reader. Aliquots were stimulated at 125°C for 20 seconds, simultaneously the energy was measured that is released during the stimulation.

The accordingly measured OSL signal decays in a few seconds (Figure 3.3). Only a component of the signal is used for equivalent dose calculations; the net signal, used for D_e calculation, is obtained by subtracting a background signal from the initial signal (Murray and Wintle 2000).

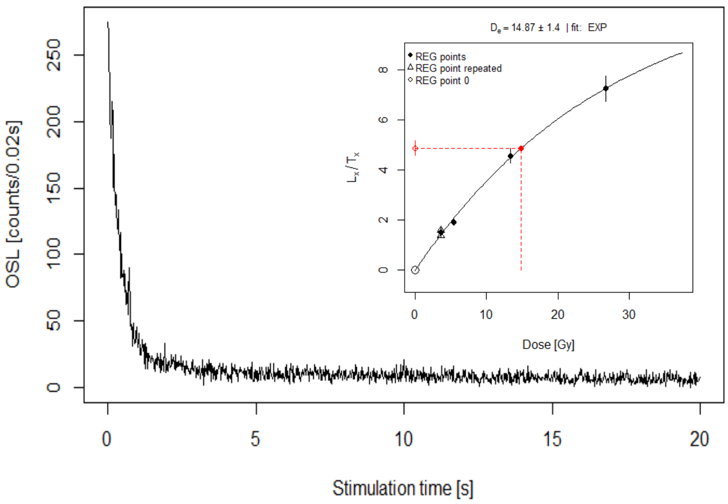

Figure 3.3. Quartz decay curve and regenerated growth curve of sample A52_80. Measurement with aliquot size of 2 mm (~49 grains). First 0.48s as initial signal, 0.48-1.76s as early background.
Black dots are the regenerated dose-rates, hollow triangles are the repeated regenerated dose-rates, the latter are not used in calculating the growth curve. The curve fitting is exponential.

The *fast* OSL component is the most suitable for dating, as it is rapidly bleached and less influenced by thermal transfer (Wintle and Murray 2006). To maximise the contribution of the fast OSL component to the net OSL signal, which is the difference between the initial signal and the background signal, the early background approach was used (Cunningham and Wallinga 2010). The initial signal in this study was 0-0.48 seconds and the background signal 0.48-1.76 seconds.

The samples were analysed using the single-aliquot regenerative-dose (SAR) protocol (Murray and Wintle 2000).

The key element of the SAR protocol (see Table 2) is that a single aliquot is used for regenerative dose measurements to calculate the natural dose. After each natural or regenerative OSL measurement, a small test dose is given to the aliquot which remains constant during the entire analysis. Sensitivity changes during the measurement can be analysed and corrected for by use of this test dose.

To correct for sensitivity changes, the natural OSL (L_n) or regenerative dose (L_x) is divided by the test dose response (T_n or T_x for natural and regenerative dose respectively) (Murray and Wintle 2000). The given dose-rates and their corresponding L_x/T_x ratios can be used to calculate the natural dose, like the growth curve shown in Figure 3.3. To calculate the natural dose, the growth curve is fitted exponential and forced through the origin, as grains with zero dose should give zero signal.

Table 2. Generalised single-aliquot regeneration sequence, by Murray and Wintle (2003). The L_i and T_i are derived from the original OSL signal minus a background value of the first 0.48s and the next 1.28s respectively

Step	Treatment	Observed
1	Give Dose (or natural for first series)	
2	Preheat to 200°C for 10s	
3	Stimulate at 125°C for 20s	L_i
4	Give test dose	
5	Heat to 180C	
6	Stimulate at 125°C for 20s	T_i
7	Hot bleach at 210°C for 40s	
8	Return to step 1	

$$y = a(1 - \exp\left(-\frac{x+c}{b}\right) + g * x \quad (3)$$

The exponential equation fitted to the dose response curve data, with y the L_x/T_x ratio and x the dose [Gy] (Duller 2015).

The test doses of each regenerative measurement are compared to check for any sensitivity changes during the measurement cycle. As additional check the first regenerative dose is repeated two times, after which the Lx/Tx ratios are compared. The ratio of the 1st and the repeated regenerative doses is called the recycling ratio. The results of the measurements were analysed using Analyst 4.31.7 by Duller (2015), Rstudio with additional Luminescence package and Matlab.

The following acceptance criteria were maintained to select aliquots and calculate L_x/T_x ratios:

- The recycling ratio may not exceed 15%.
- The uncertainty in the test dose must be lower than 15%, or 20% for 1mm aliquots (max. test dose error).
- The net signal of the natural (minus background) has to be more than three times the sigma of the background signal.

Grains were mounted on stainless steel discs using silicon oil spray. The size of the mask used to spray the silicon oil on the disk, and thus also the corresponding number of grains, is called the aliquot size. The samples of this study are relatively young, origin from a small catchment and have a high chance of not being fully bleached. To analyse the D_e distribution properly and not overestimate the sediment age, the measurements have been carried out on small aliquots.

Measuring small aliquots (1-2 mm) allows the distribution of D_e to be characterised and is much less time consuming than measuring actual single grains (Duller 2008; Fuchs and Lang 2009). Lüthgens et al. (2011) concluded from a single grains analysis of Weichsel glaciofluvial sediments in NE Germany, only 2.8 to 5.0 % of the grains are accepted for calculating the equivalent dose. Similar observations were made by Reimann et al. (2012) for beach sediments which were directly derived from a Saalian push-moraine on the North Sea island Sylt (N Germany). Accordingly, small aliquots can be a reliable proxy for single-grain dose distribution as most of the signal will arise from a single to a few grains (Reimann et al. 2012).
For measuring D_e, a relatively coarse grain size (212-250 µm) has been used since coarse grains often appear to be better bleached (Olley et al. 1998); also the number of grains per aliquot can be better controlled with coarser grains.

An aliquot size of 2 mm is used for this study, which is on average 49 ± 16 grains per aliquot. To estimate the amount of grains (n) per disc equation two was used (Heer et al. 2012):

$$n = (\pi * x^2)/(\pi * y^2) * d \qquad (2)$$

With x the diameter of the aliquot size [microns], y the mean grain size [microns] and d the mean packing density which is assumed to be 0.65.
For two samples, A50_58 and A51_68, additional measurements were done with a mask size of 1 mm, ~12 ± 6 grains per aliquot, to check whether there are no *phantom doses* measured (Arnold and Roberts 2009); if two or more grains of one aliquot react with significantly different doses, the result will be an average which is no actual existing dose. For example a dose of 1 Gy and 10 Gy gives 5.5 Gy. To be able to characterise the distribution of the equivalent doses, at least 48 aliquots were measured per sample.

For dose-rate estimations, the activity concentrations of ^{40}K, ^{210}Pb, ^{212}Pb, ^{214}Pb, ^{212}Bi, ^{214}Bi, ^{228}Ac and ^{234}Th isotopes were measured. From these concentrations the total dose-rates were calculated using the conversion factors of Guérin et al. (2011). To calculate the effective dose-rate, depth, organic content, water content and grain size are taken into account (Aitken 1985). Also cosmic dose-rate is included following Prescott and Hutton (1994), for which gradual burial is assumed.
In these dose-rate measurements additionally Caesium (Cs-137) is measured. Caesium is one of the most widely recognized radioactive isotopes, produced as a result of nuclear weapons testing following WWII. There are no natural sources that produce Caesium, and its first measurable increase in atmospheric concentration on the northern hemisphere was in 1954 AD (Ritchie and McHenry 1990; Zalasiewicz et al. 2015). Cs-measurements can thus be used to date recent sediments and can provide an additional age check for the OSL dating of young sediments.

3.3.1. <u>Performance testing</u>

The suitability of the quartz grains for the SAR D_e determination was checked by a dose recovery test and a thermal transfer test: A dose recovery test is done to confirm the suitability of the chosen measurement protocol and a thermal transfer test is performed to avoid that the heat treatment causes transfer of charge into the OSL trap and thus will lead to D_e overestimation.

For each sample in the dose recovery test and the thermal transfer test at least 3 aliquots were measured, with a mask size of 5 mm. For the dose recovery test, a dose of 1.1 Gy was given to each sample, except for one sample, A53_95, a dose of 10.7 Gy because of its expected older age. If the *measured dose / given dose* ratios are close to 1, the chosen measurement protocol is suitable. The results show all the recycling ratios are close to unity, with an average of 0.98 (n=84) (Figure 3.4).

For the thermal transfer test, sample B42_20 and A49_50 were bleached and subsequently measured at different preheat temperatures for 10 seconds in a range of 180 to 280°C. Figure 3.5 demonstrates that the grains are independent of preheat temperature in a range of 180 to 220°C. For this study a preheat temperature of 200°C and a cut heat of 180°C were used.

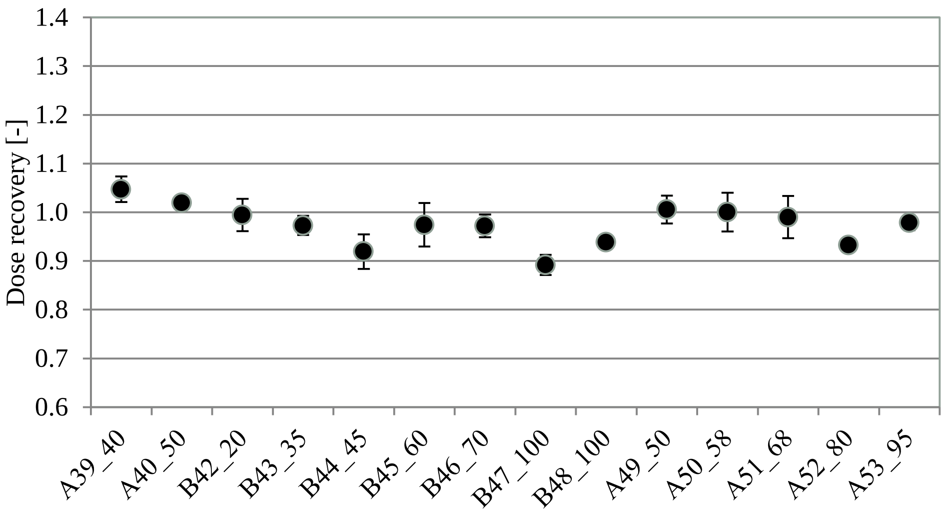

Figure 3.4. Dose recovery test for all the samples, the samples are given a known dose, which is measured afterwards. The given dose is divided by the measured dose. 3 discs were measured per sample. The average dose recovery is 0.98 (n=84)

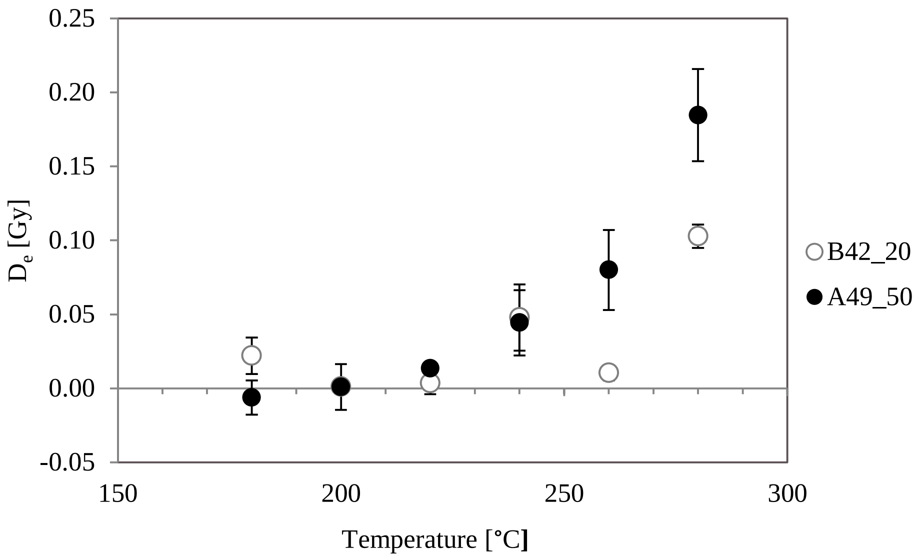

Figure 3.5. The results of a thermal transfer test, which show the influence of the preheat temperature. Equivalent dose is plotted against increasing preheat temperature, the electron traps are emptied first by stimulating the grains twice with a blue LED

3.3.2. D_e and age determination

To determine the actual burial age of the samples, the central and minimum age models (CAM and MAM) of Galbraith et al. (1999) were used. These models are essential to estimate the true paleodose. In these age models the input data are the estimated natural logarithms of the paleodoses and their standard error respectively $\widehat{\delta_i}$ and s_i for i=1,2,...,n. The central model yields:

$$\widehat{\delta_i} = \delta_i + \epsilon_i$$

The estimated paleodose $\widehat{\delta_i}$ has a random deviation of ϵ_i from the true paleodose δ_i. ϵ_i is a random quantity with mean 0 and standard deviation s_i

The measured paleodoses (δ_i) are assumed to be drawn from a normal population with exp(μ) and σ as mean and standard deviation respectively. The principle of this model is that the true doses vary randomly with a lognormal distribution. The estimated σ is multiplied by 100 and called the *overdispersion*, which represents the explained variation in paleodoses. Both models use a weight depending on the standard error of the individual paleodose measurements.

If a sample is partially bleached, the distribution of D_e values will be positively skewed and truncated around the age of the fully bleached grains. In the case of partially bleached sediments, the minimum age model provides the best estimate for the true burial age. The minimum age model estimates the burial age to be close to the age where the distribution is truncated.

Because the samples in this study are relatively young and can contain even negative paleodoses, taking a lognormal of the paleodose is often impossible. For these very young samples, un-logged versions of these age models have been used (hereafter denoted as CAMul and MAMul), which have been revised and tested by Arnold et al. (2009).

The decision of using the CAM or MAM depends on sample characteristics; if a sample is well bleached, the central age model is assumed to give the best age estimate. When a significant number of the grains is partially bleached, and thus the measured D_e values are widely spread, the minimum age model is more suitable (Galbraith et al. 1999).

In this study, the burial ages are relatively low or sometimes even negative and most samples contain partially bleached grains. Taking the central age would result in an overestimation of the burial age. Only the aeolian coversand deposits are expected to have been fully bleached at time of deposition. So the central age model is only applied to this sample, A53_95. The minimum age model is applied to the remaining samples to provide the optimal age estimates.

The age estimations were calculated in MATLAB with a bootstrap version of the above-mentioned age models (Cunningham and Wallinga 2012). For the minimum age model the overdispersion (σ_b) needs to be estimated before the model can be run, which in this case represents the overdispersion the samples would have had if they would have been well bleached (Cunningham et al. 2011). An overestimate of σ_b will lead to an overestimation of the burial dose and an underestimate of σ_b vice versa (Cunningham and Wallinga 2012). To estimate the overdispersion, the Central Age Model (CAM) of Galbraith et al. (1999) is used to calculate the overdispersion for each sample. The overdispersions of the samples range from ~14% to ~74%. As σ_b represents the scatter in D_e from sources other than partial bleaching, the minimum age model was used to consequently calculate the best estimate of the resulting overdispersions. For this study, this resulted in an estimate of the overdispersion of 0.27 ± 0.09 %.

Half of the samples contain individual measurements that are negative within their uncertainty limits. For these samples only the un-logged version of the age models is suitable.

The logged and un-logged versions of the age models give a slightly different result when they are used to calculate age estimates for the same input data. Because the other half of the samples does not contain negative values, the best suitable age model is selected using radial plots of the samples (see Appendix B).

In four out of five times, there are more individual D_e measurements within 2 sigma of the un-logged MAM estimate than within 2 sigma of lognormal MAM estimate. The former is thus used as age model for the minimum age.

The central age model is only used for sample A53_95 which is not a young sample compared to the rest of the samples. Also, the CAM performed better than the CAMul in a radial plot.

The results of every sample are visually checked with a Kernel density plot and a radialplot (Figure 3.6). These plots can provide valuable information about the deposition situation by the degree of spread and skewness in the data.

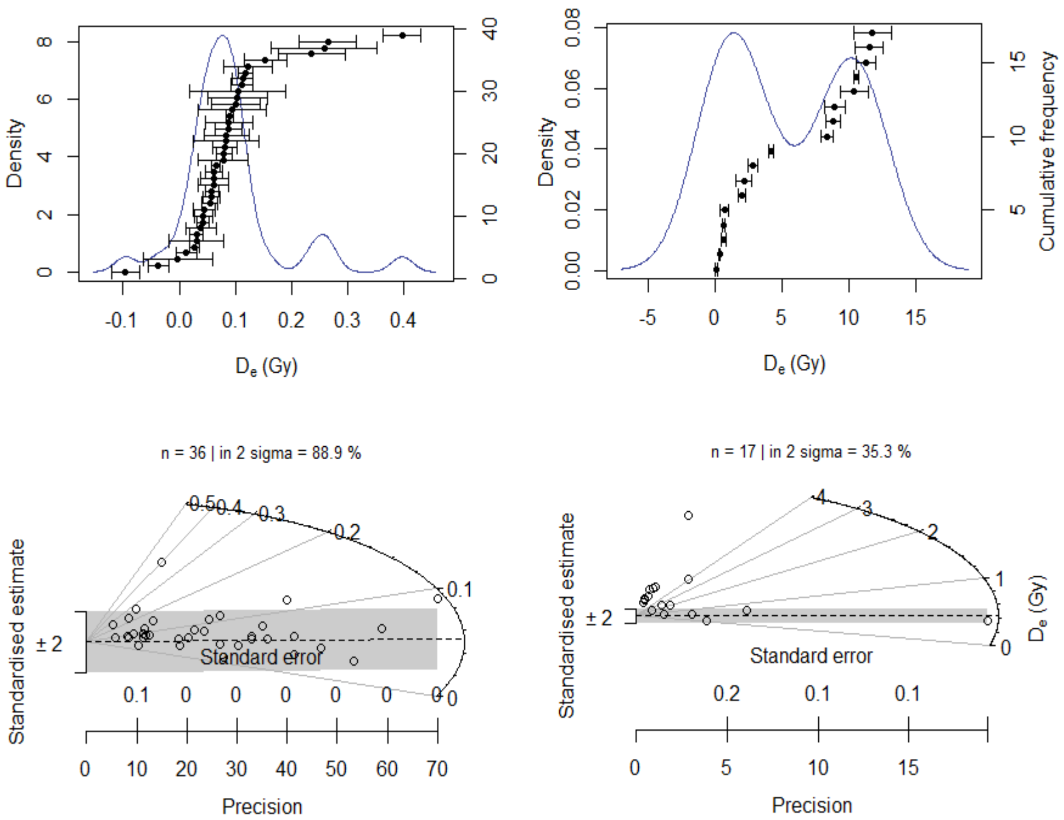

Figure 3.6. Kernel density plots (top) of two samples with different degrees of bleaching:
B43_35 (left): location B, depth 35cm, 2 mm aliquot
A51_68 (right): location A, depth 68cm, 1 mm aliquot
Both samples are partially bleached, however, sample A51_68 is more poorly bleached. Black dots are the resulting De values (Gy) per aliquot with corresponding error bars.
Radialplots (below) of the same samples. Grey bar is the 2 sigma around the MAMul age. For B43_35 88.9% of the measurements is within a 2 sigma from this age, for A51_68 this is only 35.3%

4. Results

4.1. *D_e and age results*

Equivalent doses are shown in Table 3. Only for sample A53_95, the central age model is used because this is assumed to be coversand and thus well bleached at the time of deposition. This is presumed to be the only undisturbed and fully bleached sample. The other samples are expected to have been poorly bleached, which is confirmed by the spread in D_e values and a relatively high overdispersion. For these other samples, the un-logged Minimum Age Model is used.
Sample A50_58 and A51_68 show the highest overdispersion because of the poor bleaching (see Figure 3.6).

The sediments of location B showed a higher organic matter content than location A, indicated in Table 4. The deepest samples of both locations are very low in organic matter, which is typical for an aeolian origin of the sand. However, only the lowest sample of location A has the correct age to be classified as coversand.

Caesium (^{137}Cs) was measured in the dose-rate measurements of two samples (B46_70 and B42_20) originating from a depth of 68 and 40 cm below the surface. Caesium provides an independent age check, as there are no natural sources, and the first atmospheric increase of caesium was in 1954 AD. under the assumption the Caesium is direct absorbed and has not been leached throughout the soil profile, this measurement provides an additional age check.

*Table 3. Equivalent dose D_e (Gy) and errors, dispersion, dose-rate and applied age model. The MAMul age is expected to give the most accurate estimation of true equivalent dose, except for sample B48_100 where the CAM age shows a better estimation. Caesium is measured in the samples of location B indicated with a *.*

Sample nr.	D_e (Gy)	Dispersion (Gy)	Dose-rate (Gy/ka)	Age Model
Location A				
A39_40	0.08 ± 0.02	0.08	0.9	MAMul
A40_50	0.14 ± 0.01	0.59	0.9	MAMul
A49_50	0.23 ± 0.02	0.53	1	MAMul
A50_58	0.50 ± 0.12	7.17	0.9	MAMul
A51_68	0.43 ± 0.15	7.03	0.9	MAMul
A52_80	0.48 ± 0.05	4.37	0.9	MAMul
A53_95	10.2 ± 0.4	0.16	0.7	CAM
Location B				
B42_20*	0.05 ± 0.004	0.08	0.9	MAMul
B43_35	0.05 ± 0.01	0.08	0.9	MAMul
B44_45	0.09 ± 0.03	0.32	1.1	MAMul
B45_60	0.08 ± 0.02	0.06	1.4	MAMul
B46_70*	0.10 ± 0.01	0.11	1.4	MAMul
B47_100	0.13 ± 0.01	0.01	1.2	MAMul
B48_100	0.24 ± 0.03	2.74	0.9	MAMul

*Table 4. OSL estimated burial ages and errors. Caesium is measured in the samples of location B indicated with a *.*

Sample nr.	Age (ka)	Depth (cm)
Location A		
A39_40	0.09 ± 0.02	40
A40_50	0.16 ± 0.01	50
A49_50	0.24 ± 0.03	50
A50_58	0.55 ± 0.13	58
A51_68	0.50 ± 0.18	68
A52_80	0.56 ± 0.05	80
A53_95	14.1 ± 0.6	95
Location B		
B42_20*	0.06 ± 0.01	20
B43_35	0.06 ± 0.01	35
B44_45	0.08 ± 0.03	45
B45_60	0.06 ± 0.01	60
B46_70*	0.07 ± 0.01	70
B47_100	0.11 ± 0.01	100
B48_100	0.27 ± 0.03	100

4.2. ***D_e* distribution and scaling**

The distribution of individual D_e values, as shown in Figure 4.1, provides the possibility to visually check the sample characteristics. The samples with a higher degree of partially bleaching show a broader distribution of D_e values. Two samples of sample location A, A50_58 and A51_68, were first measured on 2 mm aliquots and later on 1 mm aliquots to improve the accuracy of the age estimation (Figure 4.). The results of the 1 mm aliquot fit better in the deposition chronology, and the error in age estimation improved significantly.

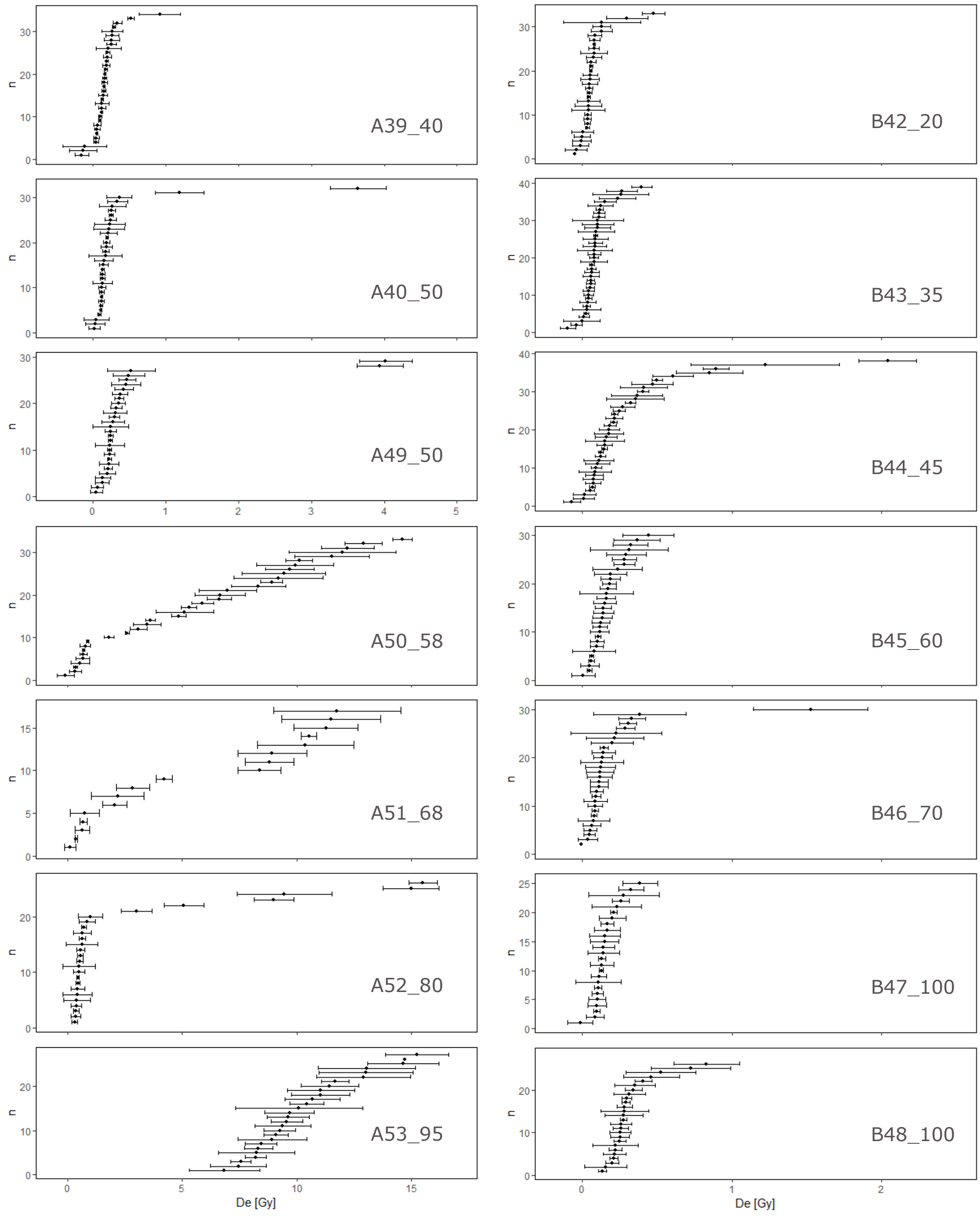

Figure 4.1. D_e distributions, sorted by increasing depth. Left: location A, right: location B. The axis of the left column is different for the lower 4 graphs. Difference in bleaching degree is clearly visible between the samples.

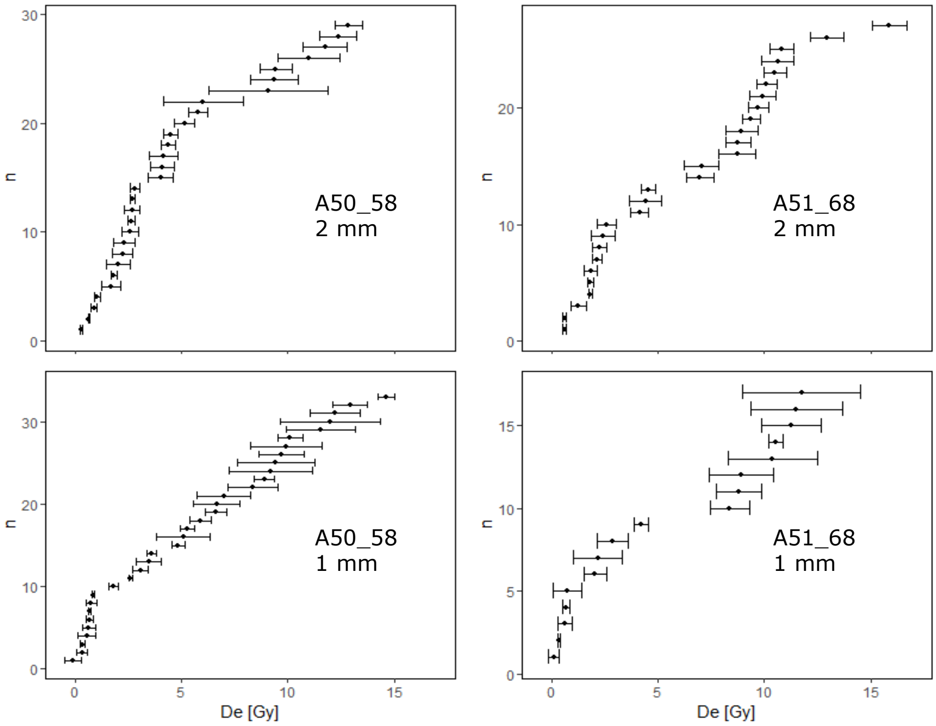

Figure 4.2. Sample A50_58 (left) and A51_68 (right) on 2 mm (top) and 1 mm (bottom) aliquot sizes. The MAMul age changed from 0.41 ± 0.23 ka and 0.64 ± 0.32 ka to 0.50 ± 0.18 ka and 0.56 ± 0.05 ka respectively.

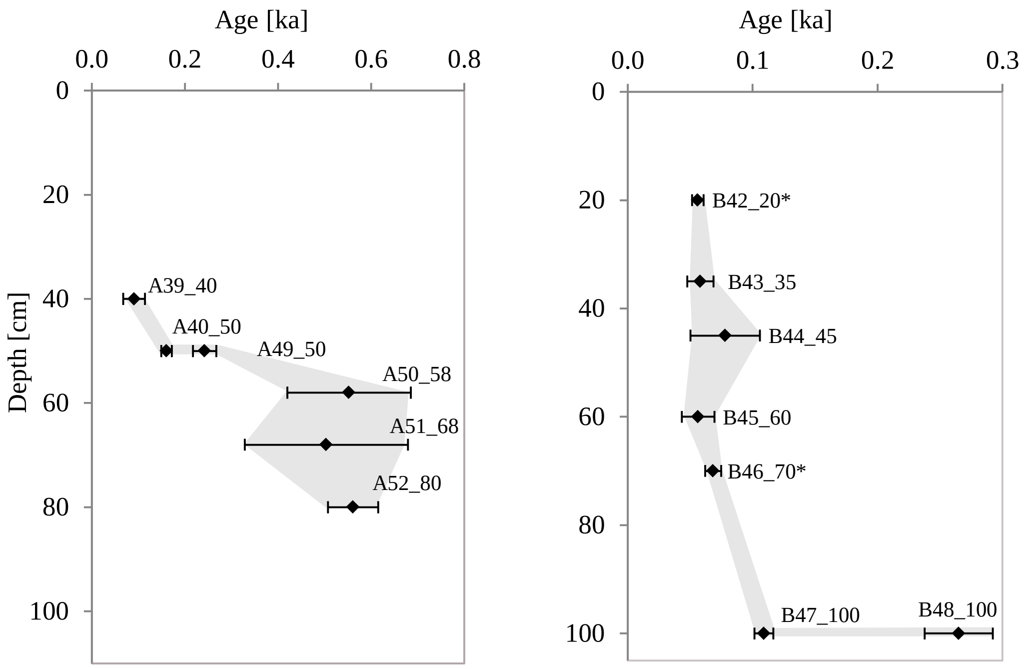

*Figure 4.3. OSL age - depth. Left: location A, Right: location B. The grey area indicates the uncertainty around the measurements. Caesium is measured in the samples of location B indicated with *. To fit the scale of the left graph, sample A53_95 is not shown.*

5. Discussion

Since the last decades, OSL dating has been used regularly for the dating of colluvium. For timing of past soil erosion, OSL dating is the most suitable compared to indirect dating techniques like radiocarbon dating (Fuchs and Lang 2009). Although OSL dating is an accurate method for dating colluvium (Fuchs and Lang 2009; Fuchs et al. 2010; Poręba et al. 2011), the soil erosion and deposition distances are rather short in the small catchments of this study area which increases the chance of incomplete bleaching. As well the burial ages are young, which makes the OSL dating in this study challenging and unique. In this chapter, complications encountered during this study and interpretations are discussed.

5.1. *Dating chronology*

In OSL dating and especially of colluvium, incomplete bleaching is a common complication (Preusser et al. 2008). Most samples in this study are colluvial sediments originating from a small catchment, with gentle slopes. The catchment areas upstream of the sample locations are 2.2 km^2 and 0.8 km^2 for respectively location A and B, with an average slope of 2°. Because for small catchments the erosion-deposition distances are short, the chance of incomplete bleaching before burial increases.

As the chance of incomplete bleaching is high for the colluvium in this study area, the samples were analysed on small aliquots to be able to characterise the distribution of D_e values (Duller 2008). Measuring small aliquots is shown to be a good proxy for single grain measurements (Reimann et al. 2012) and is much less time consuming. Multiple aliquots were measured per sample with an aliquot size of 2 mm (~49 grains). The results from the dose recovery test indicate the quartz sediments from the study area demonstrate good behaviour for luminescence dating. Except for sample A53_95, which is assumed to be wind deposited, all the samples are expected to have been bleached incompletely at time of burial.

Two samples, A50_58 and A51_68, have a broader spread in D_e values compared to the other samples. For those two samples additional measurements have been done with 1 mm aliquots (~12 grains) to obtain a higher resolution and check whether there are no phantom doses present. The MAMul ages obtained from the 1 mm aliquots have a smaller measurement error and fit better within the chronology of the sampling results.

For the poorer bleached samples the averaging effect is bigger when a signal arises from more than one grain. By measuring on 2 mm aliquots the chance of averaging and thus age overestimation is higher compared to 1 mm aliquots. The big spread in D_e values and the high overdispersion in sample A50_58 and A51_68 are caused by incomplete bleaching or even mixing with unbleached sediments during the deposition and burial process. This could indicate erosion and deposition happened in a short timespan with poor bleaching circumstances, like deposition in very wet conditions or clumped sediments where only the outer grains have had a chance of bleaching.

The most appropriate model for estimating the burial age of incomplete bleached samples is the MAM model by Galbraith et al. (1999) (Galbraith et al. 1999; Arnold et al. 2009; Cunningham and Wallinga 2012). Because most samples contain negative D_e values within the range of the measurement error, an un-logged version of the MAM model by Arnold et al. (2009) was used. The un-logged model puts relatively more weight on the lower D_e estimates, thus the results are slightly different than the original logged version (Arnold et al. 2009).

Despite the above mentioned constraints in the measurements, the resulting OSL ages of both locations show stratigraphic consistency. The Caesium measurements provide an additional independent age control, which shows that even the youngest measurements are accurate. These two checks validate the suitability of OSL for dating colluvium.

5.2. ***Interpretation of the results***

5.2.1. Location A

The lowest sample at a depth of 95 cm, A53_95, has the characteristics of aeolian sand: well-sorted, fine sand and low in organic matter. The OSL age of 14 ka matches as well with the phases of coversand deposition during the end of the Weichsel glacial, Older Coversand II or Younger Coversand I (Hammen 1952; Vandenberghe et al. 2013).

Because the sample above, A52_80, is dated to the Middle Ages, there is a gap between the late Weichsel and the Middle Ages. The samples above, A50_58 and A51_68 are dated as well at 500 to 600 years old, but show a very broad distribution of D_e. This could indicate a rapid burial with poor bleaching circumstances, like the earlier mentioned start of hydropower and mill-damming. As the underlying sample, A52_80, is dated at around the same age as A50_58 and A51_68 but is much better bleached, this probably has been a former topsoil. This topsoil could have been deposited much earlier but is bleached by processes like bioturbation and ploughing. The measured age is the age of burial, which in this case is around the late Middle Ages. If earlier Holocene erosion and sedimentation intensities were very small, these colluvial layers could have been present in this sample but are bleached by ages of ploughing and bioturbation.

The absence of colluvium dating from the beginning of the Holocene until the Middle Ages can have several more causes:

- Colluvium of this period was present but is eroded later, either by nature or by human activity such as watermills.
- Colluvium of this period was present but is removed to be used as material for *plaggen* fertilisation.
- Agricultural land use during this period hardly triggered erosion. Consequently, there is only a very small colluvial layer that is bleached, is not measured or is even absent.
- Agricultural land use during this period triggered erosion, but deposition did not take place at the sampled locations.

The three highest samples are better bleached, which implies they have not been deposited under the same conditions. The highest sample, at 40 cm, shows an OSL age of around 90 years. As the ploughing depth is around 35 cm, ploughing could have influenced the OSL age by mixing soil.

5.2.2. Location B

Although the characteristics of the deepest sample of this location, B48_100, match well with the characteristics of aeolian sand, it is not Weichsel coversand as the OSL age is just around 300 years. Because the bottom part of the soil profile was water saturated, sampling at lower depths was not possible. However, it is feasible that Weichsel coversands can be found at lower depths that aren't sampled.

The OSL age of this lowest sample does correspond well with the date provided in the transcription of Smeenge (Diss. in progress), indicating the obligated clean-up of the streams in the area in 1770 AD.

The sediments from the surface up to a depth of 70 cm are all deposited during the same period, around 1950-1960. In a coring in January 2016, remnants of peat were found at this location at a depth of 100 to 120 cm, which makes it presumable the soil was raised to become more suitable for agricultural land use. The presence of Caesium in the dose-rate measurements indicates that the soil was raised at the earliest in 1954 AD.

5.2.3. General interpretations

Habitation and agriculture in the area of the ice-pushed ridge of Ootmarsum started early in the Holocene (van Beek et al. 2015). The presumption exists erosion and sedimentation increased during periods of stronger human impact. Several studies in undulating areas in Europe showed that periods where anthropogenic induced soil redistribution was increased have been the Neolithic, the Bronze Age, the Roman period and the Middle Ages (Lang and Hönscheidt 1999a; Lang 2003; Fuchs et al. 2004). However, not only anthropogenic land use could have induced soil erosion: Holocene climate fluctuations could have influenced soil stability as well (Leopold and Völkel 2007; Schneider et al. 2007; Dotterweich 2008).

Because catchments on the ice-pushed ridge of Ootmarsum are relatively small and the slopes are gentle, the question is whether soil erosion has been triggered at all during the Holocene and if, what has been the prominent trigger.

No colluvium was found dating from the period between the end of the beginning of the Holocene and late Middle Ages. As the results show only increased erosion since the Middle Ages, the influence of fluctuations in climate during the Holocene have not been measurable. During the late Middle Ages, from the 13th century onwards, population density and land use increased, forests were cleared on large scale and plaggen soils developed by the start of *plaggen* fertilization (Pape 1970; Van Der Woude 1983; Van Beek 2011). Around this century the water management changed significantly by the construction of watermills for hydropower (Hagens 1979).

For both sample locations, anthropogenic activity has been the cause of soil erosion and deposition. Sample A50_58 and A51_68 are deposited in the late Middle Ages and are poorly bleached, which would be the case for erosion by watermills: rapid erosion and deposition under wet circumstances in a small catchment.

The soil profiles at location A and B show the same characteristics, however, the ages are quite different. Field interpretations of both soils would suggest they are deposited in similar circumstances by a similar cause. As well the layering would be assigned to different depositional eras. From this study, it can be concluded that field interpretations of deposition chronology cannot stand on its own and should be supported by age measurements.

6. Conclusion

OSL dating with small aliquots (~49 and ~12 grains) is proven to be a convenient method for dating colluvium, even in a small catchment were sediments are bleached incompletely because of small erosion-deposition distances. The OSL ages derived with the un-logged Minimum Age Model show stratigraphic consistency and additionally, the youngest samples match well with an independent age check of Caesium (^{137}Cs).

At the two sampled valley positions, no colluvium is found dating from the period between the beginning of the Holocene and the late Middle Ages. However, this does not exclude the possibility of erosion in this period; colluvium dating from this period could have been bleached by ploughing and bioturbation, could have been eroded in a later phase either by nature or by human activity such as milling or could have been removed for the usage of plaggen fertilisation.

The MAMul ages show that erosion-rates were high during the Middle Ages. Anthropogenic land use reached a climax around these centuries, with an increasing population density, extensive deforestation, the start of plaggen fertilisation and the construction of watermills. As follows, the causative factor for soil erosion in this period has been anthropogenic land use.

Considering the most poorly bleached samples at one of the sample locations, close to an old watermill, are dated to the late Middle Ages, the start of milling had considerable influence on the local geomorphology.

7. Recommendations

Colluvial layers can give valuable information about the history of land use or climate. In this study, the increased human activity since the late Middle Ages have had much influence on these small valley systems. It is possible erosion is triggered by land use in the Holocene in the period before the Middle Ages but the colluvium is eroded or bleached. The extent of this study area is limited to the close surrounding of the two sampled valley positions. However, as human influence is and has been big since the Middle Ages, it will be difficult to find areas that have not been influenced these last centuries. The sampled valley positions show OSL ages of soil redistribution of 260 and 600 years and at two other visited valleys the soil was probably reworked even more recently.

From this study it is not possible to conclude that there was no erosion and deposition in the period before the Middle Ages. To gain more certainty, locations should be sought further away from Plaggic Anthrosols and watermills. It could be possible that larger colluvial layers are present lower on the ice-pushed ridge, or even more in the direction of the stream outlet the Dinkel, which are less vulnerable for bleaching or erosion and sedimentation by local processes.

Acknowledgements

Over the past half year, I received help and support of several people without which I would not have been able to complete my MSc thesis. Therefore I would like to thank the following people:

First of all my supervisor, Tony Reimann, for offering the opportunity for this master thesis, for the help and support, and for discussing the results and providing the positive feedback.
My second supervisor Jeroen Schoorl for the sampling, for sharing your knowledge, discussing the results, and for supervising me and providing feedback on the report.

The NCL-staff and especially Alice Versendaal and Erna Voskuilen for introducing and demonstrating the OSL measurement procedures and for the assistance in the NCL lab.
Arnaud Temme for the pre-research and the sampling, and for sharing your knowledge and discussing the results.
Roy van Beek and Harm Smeenge for discussing my results and providing me with their knowledge about the study area and the historical framework.
Ellen for joining me on fieldwork on a snowy day in January, and for the daily discussions during the coffee breaks.
Finally I would like to thank my family and friends and especially my girlfriend Femke for always supporting me when I was stressed or had some difficulties during my master thesis.

References

Aitken, M. J. 1985. *Thermoluminescence dating*: Academic press.

Arnold, L. J., and R. G. Roberts. 2009. Stochastic modelling of multi-grain equivalent dose (De) distributions: Implications for OSL dating of sediment mixtures. *Quaternary Geochronology* 4 (3): 204-230.

Arnold, L. J., R. G. Roberts, R. F. Galbraith, and S. B. DeLong. 2009. A revised burial dose estimation procedure for optical dating of youngand modern-age sediments. *Quaternary Geochronology* 4 (4): 306-325.

Augustsson, A., M.-J. Gaillard, P. Peltola, F. Mazier, B. Bergbäck, and T. Saarinen. 2013. Effects of land use and climate change on erosion intensity and sediment geochemistry at Lake Lehmilampi, Finland. *The Holocene* 23 (9): 1247-1259.

Bouman, M. T. I. J., J. A. A. Bos, and R. van Beek. 2013. Van wildernis naar cultuurlandschap: Een reconstructie van de regionale vegetatieontwikkeling van Twente in het Holoceen.

Cunningham, A. C., and J. Wallinga. 2010. Selection of integration time intervals for quartz OSL decay curves. *Quaternary Geochronology* 5 (6): 657-666.

———. 2012. Realizing the potential of fluvial archives using robust OSL chronologies. *Quaternary Geochronology* 12: 98-106.

Cunningham, A. C., J. Wallinga, and P. S. J. Minderhoud. 2011. Expectations of scatter in equivalent-dose distributions when using multi-grain aliquots for OSL dating. *Geochronometria* 38 (4): 424-431.

Dotterweich, M. 2008. The history of soil erosion and fluvial deposits in small catchments of central Europe: Deciphering the long-term interaction between humans and the environment — A review. *Geomorphology* 101 (1–2): 192-208.

Downward, S., and K. Skinner. 2005. Working rivers: the geomorphological legacy of English freshwater mills. *Area* 37 (2): 138-147.

Duller, G. A. T. 2008. Single-grain optical dating of Quaternary sediments: why aliquot size matters in luminescence dating. *Boreas* 37 (4): 589-612.

Duller, G. A. T. 2015. The Analyst software package for luminescence data: overview and recent improvements. *Ancient TL* 33 (1): 35-43.

Food, and A. O. o. t. U. Nations. 2006. *World Reference Base for Soil Resources, 2006: A Framework for International Classification, Correlation and Communication*: Food and Agriculture Organization of the United Nations.

Fuchs, M., M. Fischer, and R. Reverman. 2010. Colluvial and alluvial sediment archives temporally resolved by OSL dating: Implications for reconstructing soil erosion. *Quaternary Geochronology* 5 (2–3): 269-273.

Fuchs, M., and A. Lang. 2009. Luminescence dating of hillslope deposits—A review. *Geomorphology* 109 (1–2): 17-26.

Fuchs, M., A. Lang, and G. A. Wagner. 2004. The history of Holocene soil erosion in the Phlious Basin, NE Peloponnese, Greece, based on optical dating. *Holocene* 14 (3): 334-345.

G. Ebbers, H. v. h. L., and R.Visscher. 1992. Bodemkaart van Nederland 1:50000, Toelichting bij kaartblad 28 oost -29 Almelo Denekamp. Arnhem: Van der Wiel B.V.

Galbraith, R. F., R. G. Roberts, G. M. Laslett, H. Yoshida, and J. M. Olley. 1999. OPTICAL DATING OF SINGLE AND MULTIPLE GRAINS OF QUARTZ FROM JINMIUM ROCK SHELTER, NORTHERN AUSTRALIA: PART I, EXPERIMENTAL DESIGN AND STATISTICAL MODELS*. *Archaeometry* 41 (2): 339-364.

Gans, W. d. 1983. Fossiele permafrostverschijnselen in Nederland. *Grondboor en Hamer* 6: 175-184.

García-Ruiz, J. M. 2010. The effects of land uses on soil erosion in Spain: A review. *CATENA* 81 (1): 1-11.

Guérin, G., N. Mercier, and G. Adamiec. 2011. Dose-rate conversion factors: update. *Ancient TL* 29 (1): 5-8.

Hagens, H. 1979. *Molens, mulders, meesters: negen eeuwen watermolens in de Gelderse Achterhoek, Salland en Twente*: Smit van 1876.

Hammen, v. d. T. 1952. Late-glacial flora and periglacial phenomena in the Netherlands. *Leidse Geologische Mededelingen* 17 (1): 71-183.

Heer, A. J., G. Adamiec, and P. Moska. 2012. How many grains are there on a single aliquot? *Ancient TL* 30: 9-16.

Jongmans, A. G., M. W. van den Berg, and M. P. W. Sonneveld. 2012. *Landschappen Van Nederland: Geologie, Bodem En Landgebruik*: Enfield Pub & Distribution Company.

Kalis, A. J., J. Merkt, and J. Wunderlich. 2003. Environmental changes during the Holocene climatic optimum in central Europe - human impact and natural causes. *Quaternary Science Reviews* 22 (1): 33-79.
Kolstrup, E. 2007. Lateglacial older and younger coversand in northwest Europe: chronology and relation to climate and vegetation. *Boreas* 36 (1): 65-75.
Koomen, A. J. M., and G. J. Maas. 2004. Geomorfologische Kaart Nederland (GKN); achergrondsdocument bij het landsdekkende digitale bestand. *Alterra-rapport* 1039 (38): 13.
Lang, A. 2003. Phases of soil erosion-derived colluviation in the loess hills of South Germany. *CATENA* 51 (3–4): 209-221.
Lang, A., and S. Hönscheidt. 1999a. Age and source of colluvial sediments at Vaihingen-Enz, Germany. *Catena* 38 (2): 89-107.
Lang, A., and S. Hönscheidt. 1999b. Age and source of colluvial sediments at Vaihingen–Enz, Germany. *CATENA* 38 (2): 89-107.
Leopold, M., and J. Völkel. 2007. Colluvium: Definition, differentiation, and possible suitability for reconstructing Holocene climate data. *Quaternary International* 162–163: 133-140.
Lüthgens, C., M. BÖSe, and F. Preusser. 2011. Age of the Pomeranian ice-marginal position in northeastern Germany determined by Optically Stimulated Luminescence (OSL) dating of glaciofluvial sediments. *Boreas* 40 (4): 598-615.
Mücher, H. J., R. T. Slotboom, and W. J. ten Veen. 1990. Palynology and micromorphology of a man-made soil. A reconstruction of the agricultural history since late-medieval times of the posteles in the Netherlands. *CATENA* 17 (1): 55-67.
Murray, A. S., and A. G. Wintle. 2000. Luminescence dating of quartz using an improved single-aliquot regenerative-dose protocol. *Radiation Measurements* 32 (1): 57-73.
———. 2003. The single aliquot regenerative dose protocol: potential for improvements in reliability. *Radiation Measurements* 37 (4–5): 377-381.
Olley, J., G. Caitcheon, and A. Murray. 1998. The distribution of apparent dose as determined by optically stimulated luminescence in small aliquots of fluvial quartz: Implications for dating young sediments. *Quaternary Science Reviews* 17 (11): 1033-1040.
Pape, J. C. 1970. Plaggen soils in the Netherlands. *Geoderma* 4 (3): 229-255.
Poręba, G., Z. Śnieszko, and P. Moska. 2011. Some aspects of age assessment of Holocene loess colluvium: OSL and 137Cs dating of sediment from Biała agricultural area, South Poland. *Quaternary International* 240 (1–2): 44-51.
Prescott, J. R., and J. T. Hutton. 1994. Cosmic ray contributions to dose rates for luminescence and ESR dating: Large depths and long-term time variations. *Radiation Measurements* 23 (2–3): 497-500.
Preusser, F., D. Degering, M. Fuchs, A. Hilgers, A. Kadereit, N. Klasen, M. Krbetschek, D. Richter, and J. Q. G. Spencer. 2008. Luminescence dating: basics, methods and applications. *Quaternary Science Journal* 57: 95-149.
Reimann, T., S. Lindhorst, K. J. Thomsen, A. S. Murray, and M. Frechen. 2012. OSL dating of mixed coastal sediment (Sylt, German Bight, North Sea). *Quaternary Geochronology* 11: 52-67.
Ritchie, J. C., and J. R. McHenry. 1990. Application of radioactive fallout cesium-137 for measuring soil erosion and sediment accumulation rates and patterns: A review. *Journal of Environmental Quality* 19 (2): 215-233.
Schmitt, A., M. Dotterweich, G. Schmidtchen, and H.-R. Bork. 2003. Vineyards, hopgardens and recent afforestation: effects of late Holocene land use change on soil erosion in northern Bavaria, Germany. *CATENA* 51 (3–4): 241-254.
Schneider, H., D. Höfer, R. Mäusbacher, and M. Gude. 2007. Past flood events reflected in Holocene floodplain records of East-Germany. *Geomorphology* 92 (3–4): 208-219.
Smeenge, H. Diss. in progress. Dissertation in progress, not yet published.
Spek, T. 2004. *Het Drentse esdorpenlandschap: een historisch-geografisch studie. Bd 1*: Matrijs.
Van Beek, R. 2011. *Relief in Tijd En Ruimte: Interdisciplinair Onderzoek Naar Bewoning En Landschap Van Oost-nederland Tussen De Vroege Prehistorie En Middeleeuwen*: Sidestone Press.
van Beek, R., M. T. I. J. Gouw-Bouman, and J. A. A. Bos. 2015. Mapping regional vegetation developments in Twente (the Netherlands) since the Late Glacial and evaluating contemporary settlement patterns. *Netherlands Journal of Geosciences* 94 (03): 229-255.
van den Berg, M. W., and C. Den Otter. 1982. Geology and Morphology of a part of the Ootmarsum Ice-pushed Ridge. *Palaeohistoria* 24: 35-40.
Van Der Woude, J. D. 1983. A LATE MEDIEVAL CLEARING AT THE EDGE OF THE DINKEL VALLEY (EASTERN NETHERLANDS). *Acta Botanica Neerlandica* 32 (4): 313-321.

Vandenberghe, D. A. G., C. Derese, C. Kasse, and P. Van den haute. 2013. Late Weichselian (fluvio-)aeolian sediments and Holocene drift-sands of the classic type locality in Twente (E Netherlands): a high-resolution dating study using optically stimulated luminescence. *Quaternary Science Reviews* 68: 96-113.
Walker, M., and M. J. C. Walker. 2005. *Quaternary Dating Methods*: Wiley.
Walter, R. C., and D. J. Merritts. 2008. Natural streams and the legacy of water-powered mills. *Science* 319 (5861): 299-304.
Wintle, A. G., and A. S. Murray. 2006. A review of quartz optically stimulated luminescence characteristics and their relevance in single-aliquot regeneration dating protocols. *Radiation Measurements* 41 (4): 369-391.
Zalasiewicz, J., C. N. Waters, M. Williams, A. D. Barnosky, A. Cearreta, P. Crutzen, E. Ellis, et al. 2015. When did the Anthropocene begin? A mid-twentieth century boundary level is stratigraphically optimal. *Quaternary International* 383: 196-203.
Zonneveld, J. I. S. 1980. *Tussen de bergen en de zee: de wordingsgeschiedenis der lage landen*: Bohn, Scheltema & Holkema.

Appendix A

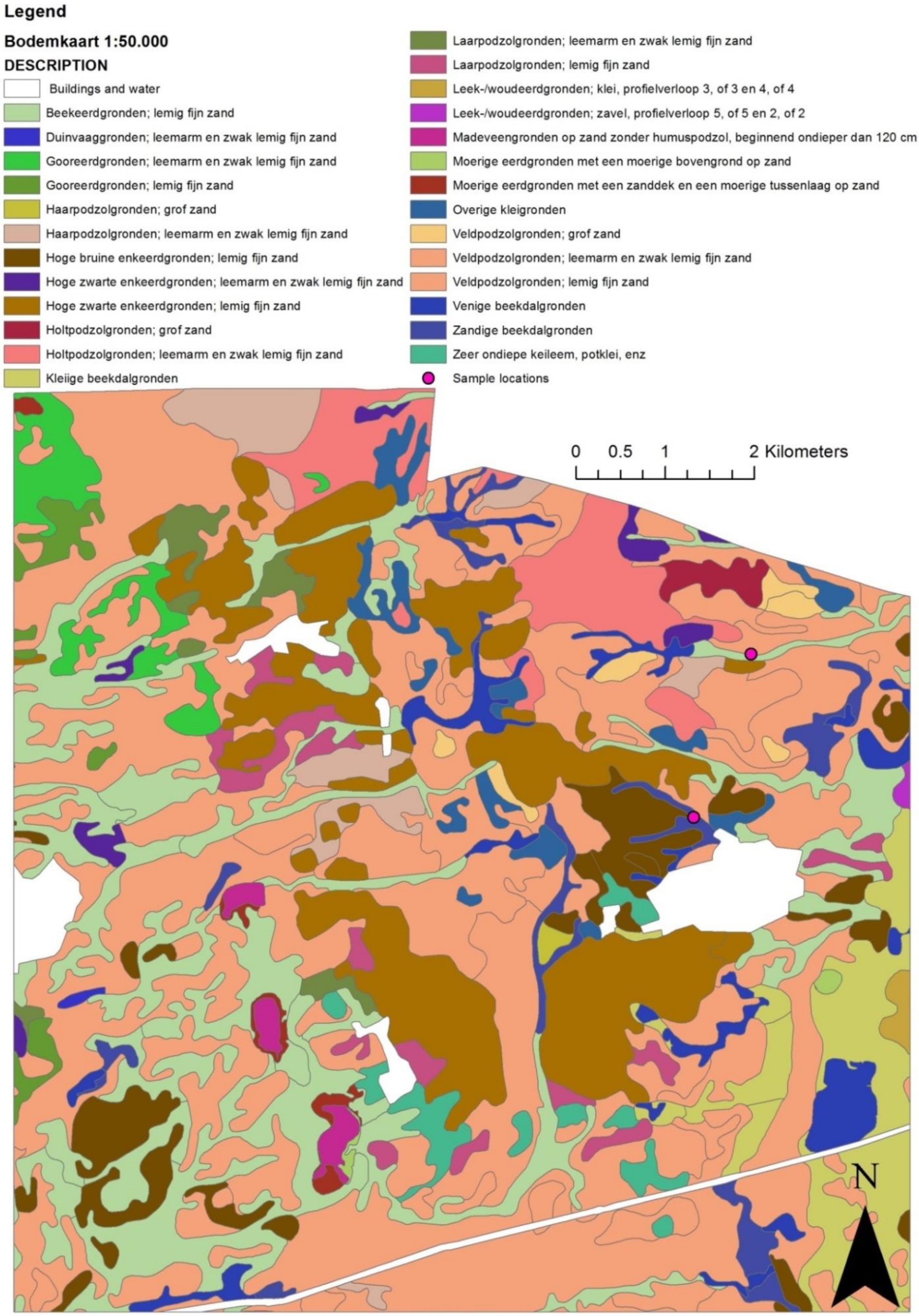

Legend
Bodemkaart 1:50.000
DESCRIPTION
Buildings and water
Beekeerdgronden; lemig fijn zand
Duinvaaggronden; leemarm en zwak lemig fijn zand
Gooreerdgronden; leemarm en zwak lemig fijn zand
Gooreerdgronden; lemig fijn zand
Haarpodzolgronden; grof zand
Haarpodzolgronden; leemarm en zwak lemig fijn zand
Hoge bruine enkeerdgronden; lemig fijn zand
Hoge zwarte enkeerdgronden; leemarm en zwak lemig fijn zand
Hoge zwarte enkeerdgronden; lemig fijn zand
Holtpodzolgronden; grof zand
Holtpodzolgronden; leemarm en zwak lemig fijn zand
Kleiige beekdalgronden
Laarpodzolgronden; leemarm en zwak lemig fijn zand
Laarpodzolgronden; lemig fijn zand
Leek-/woudeerdgronden; klei, profielverloop 3, of 3 en 4, of 4
Leek-/woudeerdgronden; zavel, profielverloop 5, of 5 en 2, of 2
Madeveengronden op zand zonder humuspodzol, beginnend ondieper dan 120 cm
Moerige eerdgronden met een moerige bovengrond op zand
Moerige eerdgronden met een zanddek en een moerige tussenlaag op zand
Overige kleigronden
Veldpodzolgronden; grof zand
Veldpodzolgronden; leemarm en zwak lemig fijn zand
Veldpodzolgronden; lemig fijn zand
Venige beekdalgronden
Zandige beekdalgronden
Zeer ondiepe keileem, potklei, enz
Sample locations
0 0.5 1 2 Kilometers
N

Table 5. English description of the most important Dutch soil types in the study area

Dutch soil classification	**English description**
Beekdalgronden	Wet soils occurring in stream valleys. Distinguished in: clayey (*kleiige-*), peaty (*venige-*) and sandy (*zandige-*).
Beekeerdgronden	Humus-rich sandy soils occurring in stream valleys. Nutrient poor coversands can be found below the Humus-rich layer.
Enkeerdgronden	Soils containing a dark humus-rich layer with a thickness of at least 50 cm. The underlying soil is most often sandy soil. The dark humus layer originates from fertilisation with manure and sods (*plaggen*). Two types of *Enkeerdgronden* occur: the *zwarte Enkeerdgrond* which contains hardly to no clay and loam and the *bruine Enkeerdgrond* which contains sand and loam
Haarpodzolgronden	Podzol with a small A-horizon, mostly developed in quartz-rich parent materials such as coversands. *Haarpodzolgronden* only occur with deep groundwater levels.
Holtpodzolgronden	Podzol with a small A-horizon, and a brown tinted B horizon.
Moerige Eerdgronden	Humus-rich soil with less than fifty percent peat within the first 80 cm but containing a peaty layer or topsoil.
Overige Kleigronden	All other clayey soils
Veldpodzolgronden	Podzol developed in the presence of high groundwater levels showing signs of gley.
Zeer ondiepe keileem	Boulderclay, close to the soil surface.

Appendix B

Table 6. Radial plots of the logged and un-logged age estimates. Left column are the un-logged models. Right column are the log scaled models. The log scaled model was not applicable when a sample contains negative values or negative values within the error range.

<table>
<tr><td>
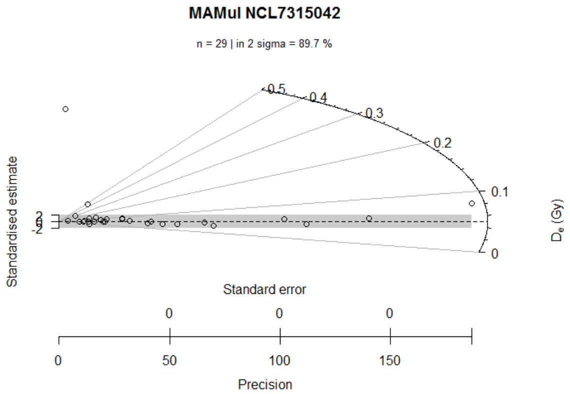

MAMul=0.05 ± 0.004 Gy
</td><td></td></tr>
<tr><td>
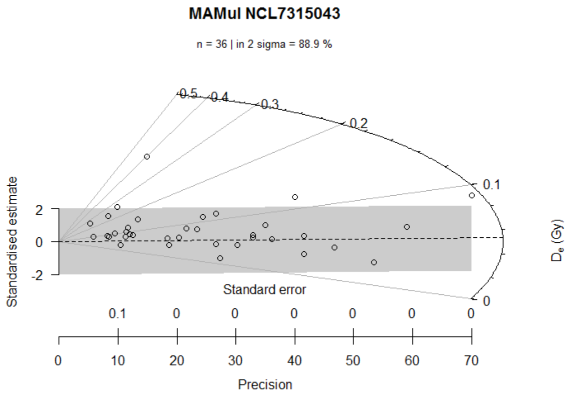

MAMul=0.05 ± 0.01 Gy
</td><td></td></tr>
<tr><td>
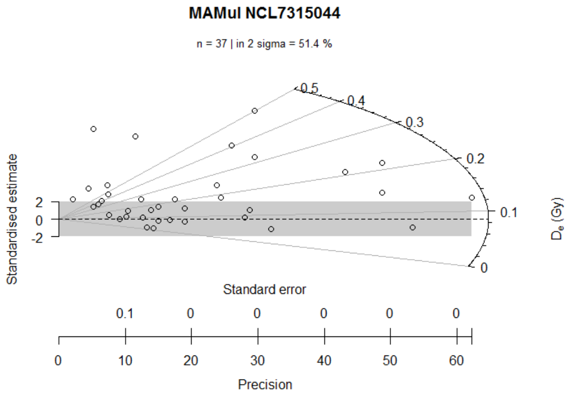

MAMul=0.09 ± 0.03 Gy
</td><td></td></tr>
</table>

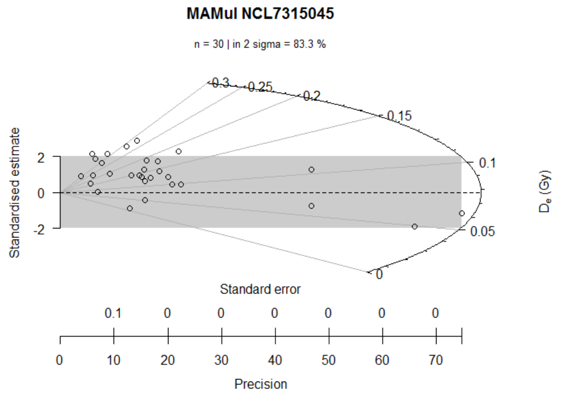

MAMul=0.08 ± 0.02 Gy

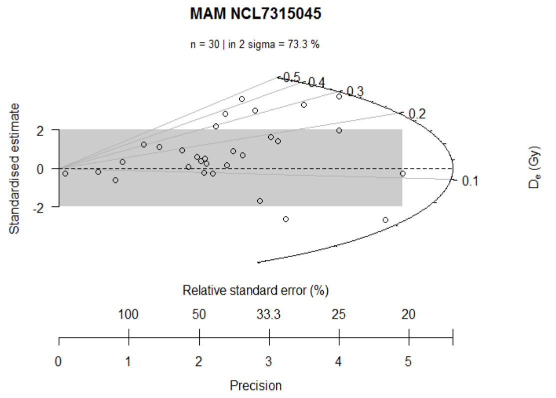

MAM=0.11 ± 0.03 Gy

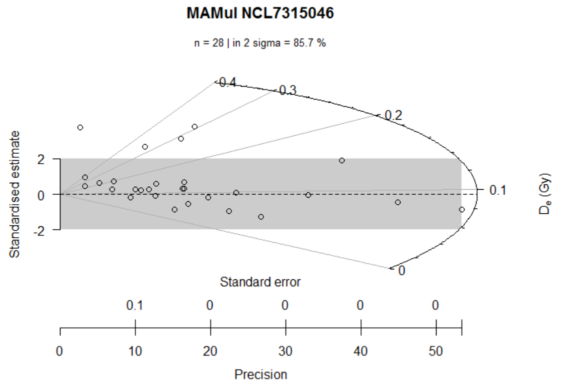

MAMul=0.10 ± 0.01 Gy

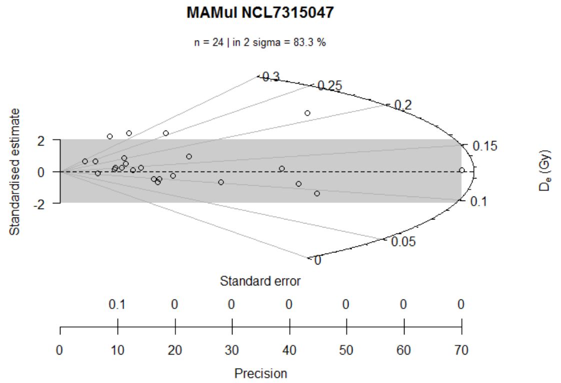

MAMul=0.13 ± 0.01 Gy

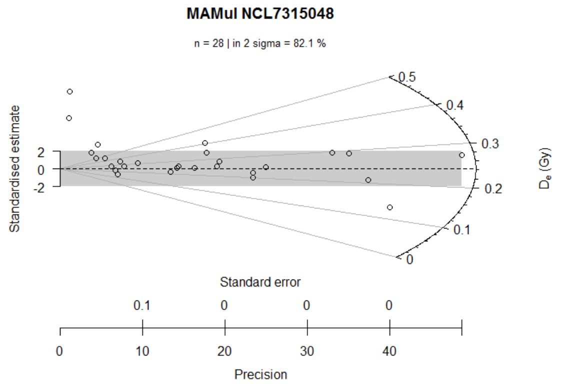

MAMul=0.24 ± 0.03 Gy

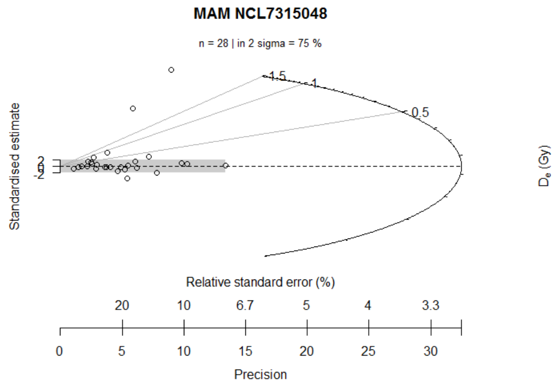

MAM=0.27 ± 0.02 Gy

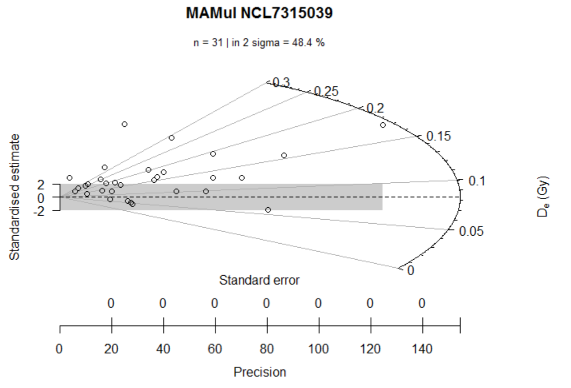

MAMul=0.08 ± 0.02 Gy

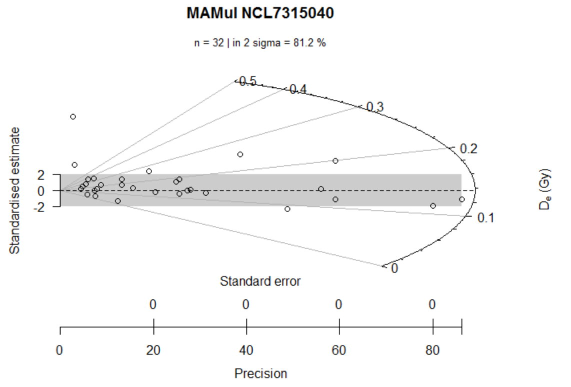

MAMul=0.14 ± 0.01 Gy

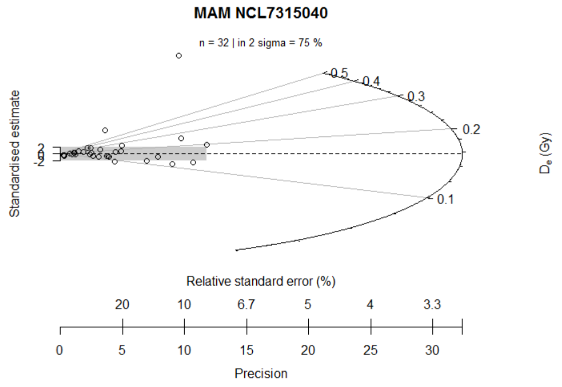

MAM=0.16 ± 0.02 Gy

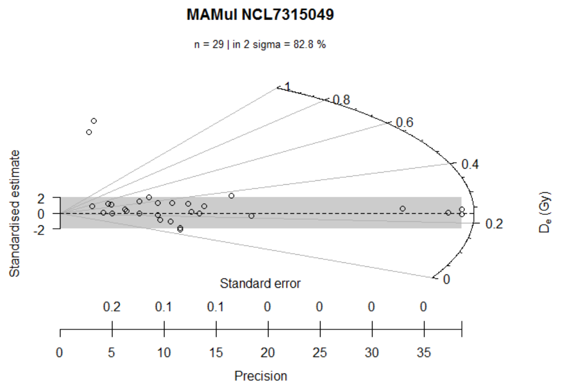

MAMul=0.23 ± 0.02 Gy

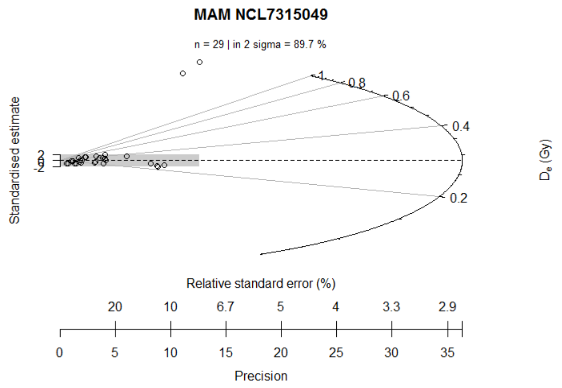

MAM=0.29 ± 0.02

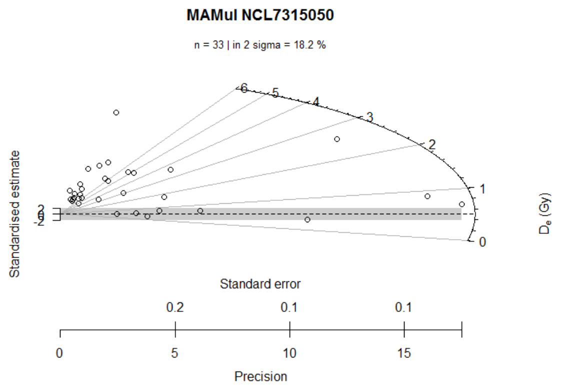

MAMul=0.50 ± 0.12

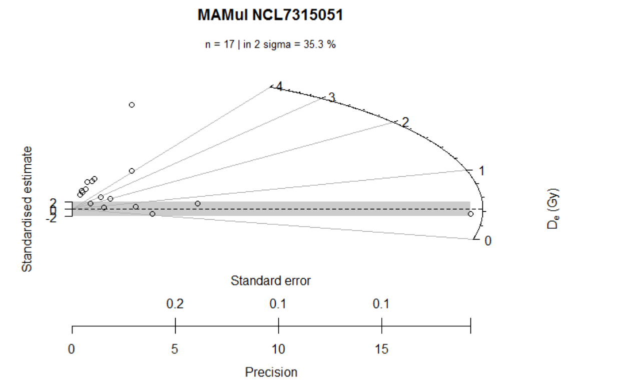

MAMul=0.43 ± 0.15 Gy

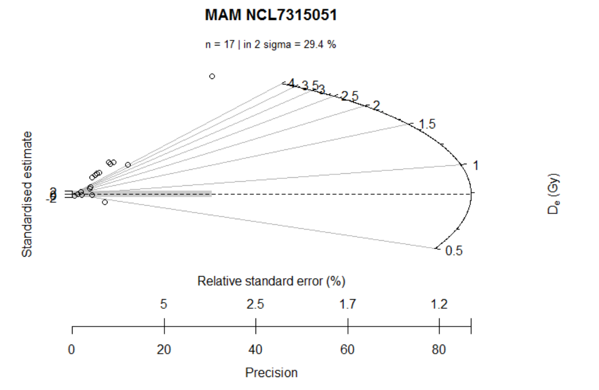

MAM=0.79 ± 0.86 Gy

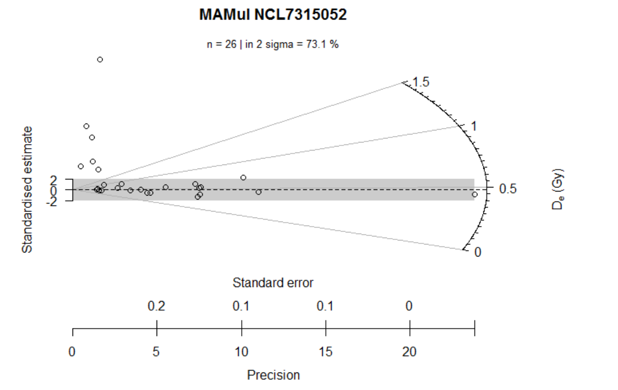

MAMul=0.48 ± 0.05 Gy

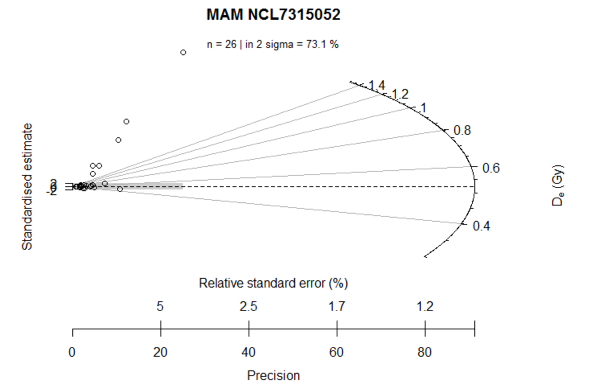

MAM=0.52 ± 0.04 Gy

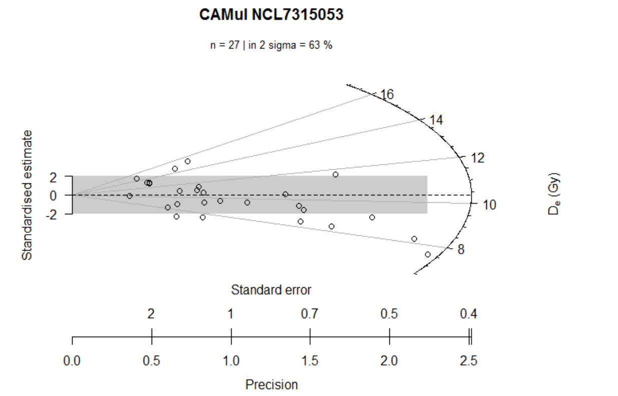

CAMul=10.3 ± 0.4 Gy

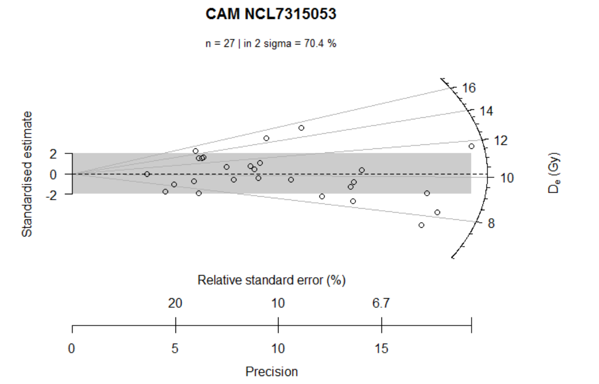

CAM=10.2 ± 0.4 Gy